Acta Crystallographica Section D
Biological Crystallography
ISSN 0907-4449

Determining the molecular-growth mechanisms of protein crystal faces by atomic force microscopy

Huayu Li,[a] Arunan Nadarajah[a]* and Marc L. Pusey[b]

[a]Department of Chemical and Environmental Engineering, University of Toledo, Toledo, OH 43606, USA, and [b]Biophysics Branch ES76, NASA/Marshall Space Flight Center, Huntsville, AL 35812, USA

Correspondence e-mail: arunan.nadarajah@utoledo.edu

Received 10 July 1998
Accepted 1 March 1999

A high-resolution atomic force microscopy (AFM) study has shown that the molecular packing on the tetragonal lysozyme (110) face corresponds to only one of two possible packing arrangements, suggesting that growth layers on this face are of bimolecular height [Li *et al.* (1999). *Acta Cryst.* D**55**, 1023–1035]. Theoretical analyses of the packing also indicated that growth of this face should proceed by the addition of growth units of at least tetramer size, corresponding to the 4_3 helices in the crystal. In this study, an AFM linescan technique was used to measure the dimensions of individual growth units on protein crystal faces as they were being incorporated into the lattice. Images of individual growth events on the (110) face of tetragonal lysozyme crystals were observed, shown by jump discontinuities in the growth step in the linescan images. The growth-unit dimension in the scanned direction was obtained from these images. A large number of scans in two directions on the (110) face were performed and the distribution of lysozyme growth-unit sizes were obtained. A variety of unit sizes corresponding to 4_3 helices were shown to participate in the growth process, with the 4_3 tetramer being the minimum observed size. This technique represents a new application for AFM, allowing time-resolved studies of molecular processes to be carried out.

1. Introduction

Many recent investigations of the crystallization of biological macromolecules have demonstrated a basic similarity to the crystallization of inorganic materials. Protein crystals can be grown by similar techniques and their growth also occurs by such processes as dislocation growth and two-dimensional nucleation growth (Durbin & Carlson, 1992; Malkin *et al.*, 1995; Malkin, Kuznetsov, Glantz *et al.*, 1996). Protein crystals themselves, however, have quite different properties to inorganic crystals. Two reasons for this difference in protein crystals are of importance in this study: the preservation of the aqueous environment in the crystalline state and the unique molecular structure of each protein, with a general lack of spatial or chemical symmetry. Both of these properties are central to the specific biological activity of each protein and its preservation in the crystalline state. These two properties can also introduce important differences in the nature of the protein crystallization process from that of small-molecule inorganic materials.

The presence of large solvent channels in protein crystals means that the environments of individual molecules in the crystal and in the solution resemble each other more than is the case for inorganic crystals. This introduces the possibility that the interactions between protein molecules in the crystalline state could also be formed in the solution state. Studies

of lysozyme solutions have suggested that not only does reversible self-association occur under crystallization conditions (Pusey, 1991; Wilson & Pusey, 1992; Behlke & Knespel, 1996; Minezaki *et al.*, 1996; Wilson *et al.*, 1996), but that the molecular arrangement of the clusters formed is similar to the arrangement in tetragonal lysozyme crystals. Enzymatic activities and other properties have indicated that they correspond to the helical arrangement of molecules about the 4_3 axes in the crystal (Wilcox & Daniel, 1954; Sophianopoulos, 1969; Zehavi & Lustig, 1971; Studebaker *et al.*, 1971; Banerjee *et al.*, 1975; Hampe *et al.*, 1982; Nadarajah & Pusey, 1996).

More significant evidence for this comes from the atomic force microscopy (AFM) investigations of McPherson and co-workers. They have shown that, unlike in the growth of small-molecule crystals, three-dimensional nucleation is a significant growth mechanism of protein and virus crystals (Malkin *et al.*, 1996*a*,*b*). In this mechanism aggregates/nuclei and microcrystals deposit from the solution on a growing face and are incorporated into the crystal. The microcrystals tend to be incorporated misaligned with respect to the crystal face, but most of the aggregates were observed to become aligned with the face. McPherson and co-workers have remarked that the number of these aggregates aligned with the underlying crystal layer is far out of proportion to what might be expected from a purely statistical basis (Malkin *et al.*, 1996*a*; Kuznetsov *et al.*, 1996). They state that this means that the aggregates must be oriented into position as they approach the crystal face or that they become aligned following deposition. Similarly, the arrangement of molecules within these aggregates must already resemble the crystalline arrangement or undergo rearrangement upon deposition.

Our investigations have further indicated that on the (110) face of tetragonal lysozyme crystals the molecular packing on the surface closely resembles, but does not exactly correspond to, the crystallographic arrangement of the crystal interior. The molecules are translated by ~7 Å and are packed closer to the 4_3 axes (Li *et al.*, 1999). This surface reconstruction or rearrangement is clearly the result of solvent interactions. This suggests that lysozyme clusters in solution may also have similar deviations from the crystallographic arrangement. If this is correct, it implies that for tetragonal lysozyme as the molecules are transferred from the solution to the bulk crystalline state some protein–protein interactions are formed in solution, while in the crystalline state these interactions relax to the precise crystallographic arrangement.

Other investigators have proposed that tetragonal lysozyme crystal growth does not involve the formation of clusters in solution. They have generally asserted that lysozyme exists solely in monomeric form in solution (Muschol & Rosenberger, 1996; Gripon *et al.*, 1997). In this mechanism, the growth of lysozyme crystals is assumed to be no different to that of inorganic ones, proceeding by the addition of individual monomers to the crystal face (Vekilov *et al.*, 1993; Vekilov & Rosenberger, 1996). However, they have not explained how growth proceeds on crystal faces where the growth steps are of bimolecular height or larger, such as the (110) face of tetragonal lysozyme and the (101) face of thaumatin crystals. Furthermore, they have suggested that lysozyme clusters could be formed in solution under certain conditions (Vidal *et al.*, 1998). Thus, these assertions are not all self-consistent and they contradict results from other studies discussed above.

An implicit assumption in standard crystal-growth theories is the uniformity of intermolecular bonds in the crystal structure. Particularly for inorganic materials, all bonds should be of equal magnitude as long as stoichiometric ratios are preserved locally. This means that these bonds do not produce a preferential pathway for crystallization. Rather, crystal growth is controlled by the formation of defects such as screw dislocations and two-dimensional nuclei for faceted growth. Growth proceeds by the preferential addition of single molecules, atoms or ions at growth sites with the highest local supersaturation and with the largest number of available molecular contacts. Non-faceted growth is solely driven by the local supersaturation. This has allowed the development of macroscopic or quasi-macroscopic growth-rate models from this classical approach to crystal growth, without taking into account any molecular considerations (Chernov, 1984).

Unlike inorganic crystals, the lack of symmetry of protein molecules results in their crystals

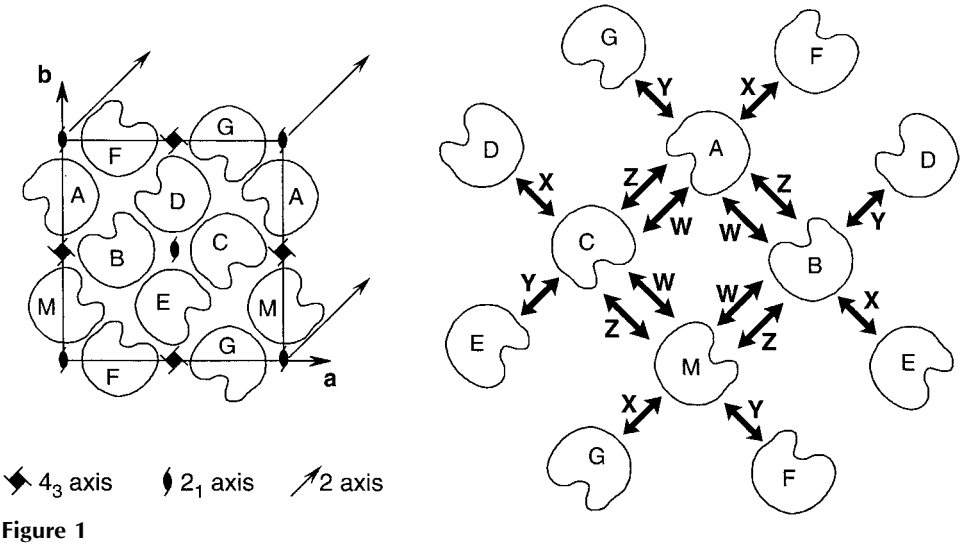

Figure 1
The unit cell and molecular interactions of tetragonal lysozyme crystals. The figure on the left shows the unit cell with a simplified representation of the eight molecules labeled *A*–*G*, with the reference molecule labeled *M*. The molecules are related to one another by the 4_3 and 2_1 screw axes as well as by the twofold symmetry axes. The figure on the right shows the four important molecular interactions labeled *W*–*Z*. The strong *W* and *Z* interaction set hold together the molecules in the 4_3 helix. A single turn of this helix is formed by the sequence *M*–*C*–*A*–*B* as shown in the figure and its twofold analog *F*–*E*–*D*–*G*. The weaker *X* and *Y* interaction set occurs between the helices.

having multiple molecular interactions. Analysis of tetragonal lysozyme crystals has shown that there are five nearest-neighbor interactions, as illustrated in Fig. 1, which have been labeled *V*–*Z*. The magnitudes of these interactions have been shown to be quite different (Nadarajah & Pusey, 1996). This introduces into the crystal structure strongly and weakly bonded molecular chains. In particular, the crystal structure can be regarded as consisting of strongly bonded molecular helices centered around the 4_3 axes, with the helices attached to each other by weaker bonds. This pronounced non-uniformity of interactions in the crystal structure affects the crystal-growth process. Growth on both the (110) and the (101) faces of tetragonal lysozyme crystals can be expected to proceed in a manner which preserves the 4_3 helices (Nadarajah & Pusey, 1996; Nadarajah *et al.*, 1997; Strom & Bennema, 1997*a*,*b*).

For protein crystals, there are molecular-level growth mechanisms in addition to the microscopic or mesoscopic growth process by dislocation and two-dimensional nucleation. In other words, growth will occur by a specific molecular process along a growth step on a dislocation hillock or a two-dimensional island on the crystal faces. Analysis of the molecular packing of the crystals by periodic bond-chain (PBC) theory has shown that this molecular process would involve the addition of lysozyme growth units of at least a tetramer in size, corresponding to the 4_3 helices (Nadarajah & Pusey, 1996; Nadarajah *et al.*, 1997; Strom & Bennema, 1997*a*,*b*). Thus, growth of these crystals would have to occur by a molecular-level process involving the formation of these growth units, followed by their addition to the crystal face by a classical growth mechanism.

However, PBC theory cannot predict whether these growth units are formed by nucleation from monomers in solution directly on the crystal face or by their formation in solution followed by their addition to the crystal face. The latter mechanism is suggested by studies showing the existence of lysozyme clusters in solution under crystallization conditions and by AFM investigations of protein crystal-growth processes described above. Additionally, modeling studies of macroscopic growth-rate data of the (110) face of tetragonal lysozyme crystals have also suggested such a process with the clusters being formed in the bulk solution (Li *et al.*, 1995; Wilson *et al.*, 1996; Nadarajah *et al.*, 1997). The former mechanism is likely to be followed if studies which claim lysozyme exists only in monomeric form in solution are correct. In this study, we will attempt to resolve these issues by observing this molecular process directly with AFM techniques.

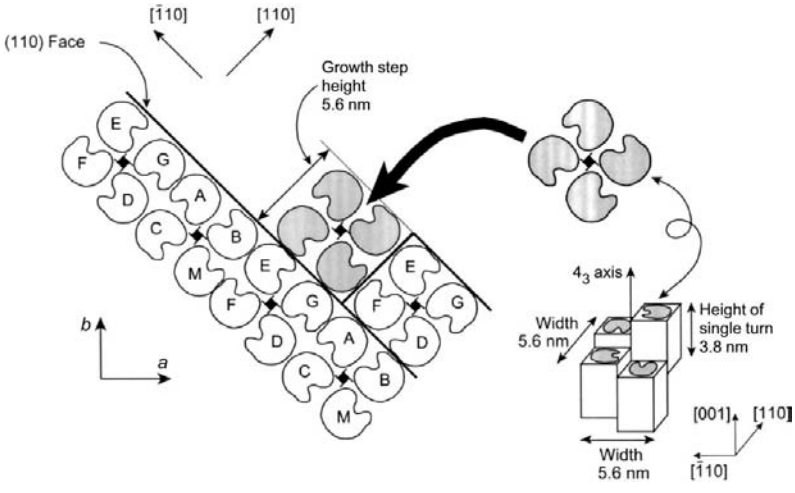

Figure 2
The structure of the (110) face and its growth steps and growth units. The molecular packing on the surface corresponds to complete 4_3 helices as shown, with growth steps which are at least bimolecular in height and corresponding to this helix. In order to fit the bimolecular step and retain the fourfold screw symmetry of the crystal, the minimum growth unit for this step must be a tetramer corresponding to a single turn of the 4_3 helix, as shown here.

2. Molecular-growth processes and their observation

Our high-resolution AFM investigations have provided direct confirmation that the molecular packing on the (110) face corresponds to complete 4_3 helices (Li *et al.*, 1999). Only the plane containing the 2_1 axes was observed in that study and not the plane containing the 4_3 axes. Since these two planes alternate in the crystal structure, the absence of the latter plane implies that growth of the (110) face must proceed by the addition of bimolecular layers, as shown in Fig. 2. If growth occurred by monolayers, then the molecular packing corresponding to the alternate plane would have been observed in the high-resolution AFM study.

If growth proceeds by bimolecular layers on the (110) face, then it suggests that the growth unit is also bimolecular in width in the [110] direction. The fourfold screw symmetry of the crystal structure would then require that the growth unit also be bimolecular in width in the [$\bar{1}$10] direction. Additionally, the growth unit must correspond to the 4_3 helix. The smallest growth unit which satisfies this requirement is a 4_3 helical tetramer (Fig. 2). Although growth by smaller units is possible, this would mean that monolayer growth steps could be formed on the (110) face. As discussed above, if monolayer growth occurs the alternate molecular-packing arrangement should have been observed on the (110) face.

The structure of a growth step on the (110) face is illustrated in Fig. 3 and shows a two-dimensional island with a characteristic oval shape caused by growth anisotropy (Nadarajah & Pusey, 1996; Nadarajah *et al.*, 1997). The [$\bar{1}$10] direction corresponds to the long axis of the island and to one width of the 4_3 helix. The [110] direction represents the growth step height as well as the other width of this helix (Fig. 2). The [001] direction in Fig. 3 corresponds to the short axis of the island and to the 4_3 axis itself. For growth by the 4_3 helical clusters, the dimension of the growth unit in the [001] direction represents the number of turns in the helix. A monomolecular length represents a single turn and a tetramer growth unit, a bimolecular length represents two turns of the helix and an octamer growth unit, and so on.

The above discussion makes clear the relationship between the growth-unit dimensions and the molecular-growth mechanism of the crystal face. If the dimensions of individual growth units could be determined, the growth mechanism can be inferred. This can be performed relatively easily for the dimension in the [110] direction, as this corresponds to the growth-unit height. Earlier investigators have already determined this by measuring the step heights (Durbin & Feher, 1990; Durbin & Carlson, 1992; Konnert *et al.*, 1994). However, in the other two directions, measuring the growth-unit dimensions would require that individual growth events be observed as they occur, which is a difficult undertaking. Even a relatively slow process such as protein crystal growth proceeds at extremely rapid rates at the molecular level under normal growth conditions.

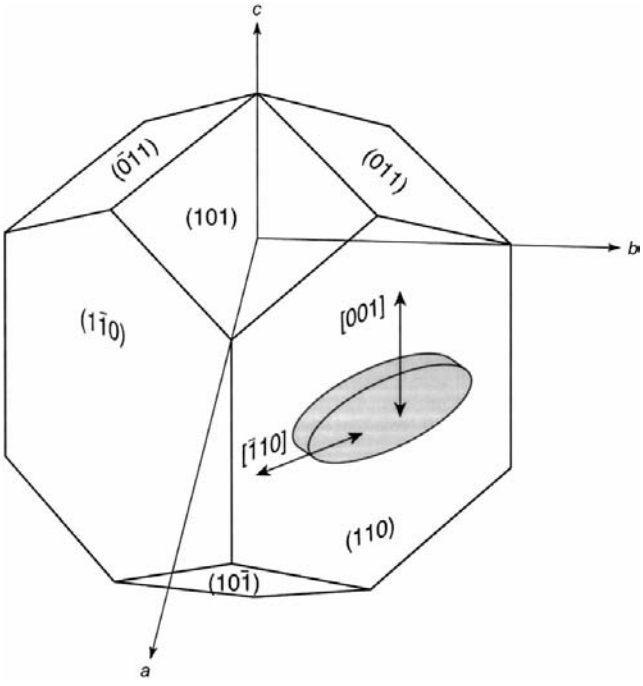

Figure 3
Illustration of a tetragonal lysozyme crystal showing the shape and orientation of two-dimensional islands which form on the (110) face during growth.

Despite the difficulty, many recent investigations have succeeded in observing molecular processes. This has been achieved in two ways: by slowing the molecular process and by employing rapid observation techniques. For example, the use of cryogenic temperatures has made it possible to slow the photolysis of the carbon monoxide complex of myoglobin in the crystalline state. This has allowed multiple images of the process to be obtained by Laue-diffraction techniques, showing the structural changes taking place (Teng *et al.*, 1994). More recently, development of a very fast Laue diffraction technique has made possible nanosecond time resolution of these same structural changes, allowing the process to be observed at ambient temperatures (Šrajer *et al.*, 1996). Similarly, the development of electron-diffraction techniques employing very short electron pulses has given rise to the field of femtochemistry (Zewail, 1996). It has enabled investigators to observe chemical reactions between individual small molecules on picosecond timescales (Williamson *et al.*, 1997).

In this study we will use both types of approaches, namely employing rapid observation techniques and slowing down the growth process, to observe individual growth events on protein crystal faces. In order to speed up the observation process, the little-used AFM linescan technique will be employed. Instead of scanning an area of the crystal face, which can take many seconds or minutes, in the linescan mode the scans are performed repeatedly on a single line, each of which can be completed in tens of milliseconds. The resulting images from linescans show the morphology of the line on one axis, while the other axis displays the time-evolution of this morphology. By selecting a line which crosses a growth step on a crystal face for scanning, the motion of the step during growth can be captured. Such scans have been carried out previously for tetragonal lysozyme crystals under normal growth conditions (Durbin & Carlson, 1992; Konnert *et al.*, 1994) and an example of one obtained in this study is shown in Figs. 4(*a*) and 4(*b*).

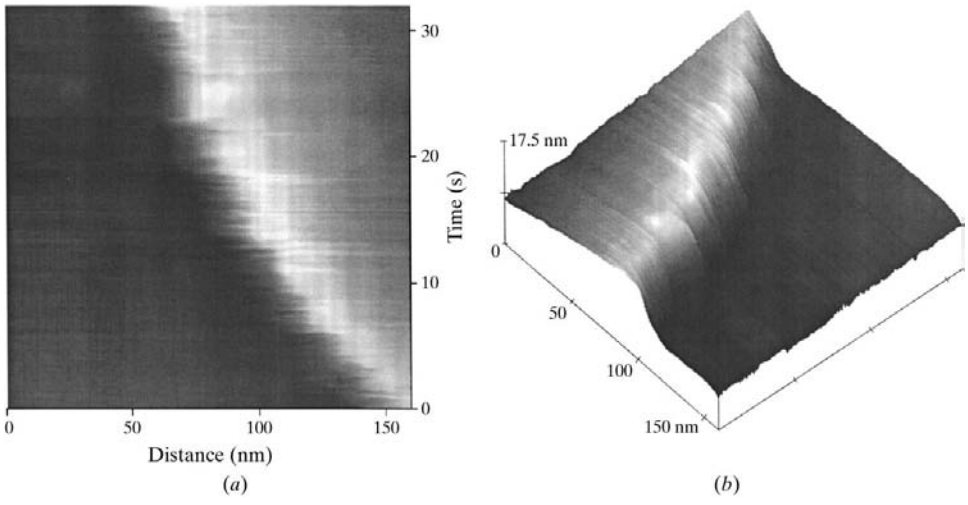

Figure 4
An AFM linescan image obtained by scanning across a growth step on the (110) face under normal growth conditions. (*a*) The two-dimensional view where only the motion of the growth step is visible. (*b*) The three-dimensional view showing, in addition to the step motion, that the growth step has a height of ~5.6 nm. The growth step moves continuously over time producing a slope in the linescan image. The gradient of this slope at any point gives the step velocity at that time.

Figs. 4(*a*) and 4(*b*) show that the motion of the step is continuous under these conditions and a macroscopic step velocity can be obtained from the slope of the curve. Thus, even in the AFM linescan mode the growth process is usually continuous and indivi-

dual growth events cannot be observed. In order to do so, the growth process must be slowed considerably. Since the growth rates of crystal faces are a function of the solution supersaturation, they can be reduced to extremely small values by appropriately decreasing the supersaturation (Nadarajah *et al.*, 1995). In this study, this was achieved by reducing the supersaturation as close as possible to the saturation limit and performing the AFM linescans. Such a linescan image for the (110) face of tetragonal lysozyme is displayed in Figs. 5(*a*) and 5(*b*). Unlike Figs. 4(*a*) and 4(*b*), these images show that the growth step is unchanged during the scan period, except at one point when a single growth event occurs and the step moves suddenly in a discontinuous manner. This can be attributed to the 'instantaneous' addition of a single growth unit from the solution to the growth step. ('instantaneous' here means a process faster than the time resolution of this technique, *i.e.* less than 10 ms). By measuring the distance moved by the step, the dimension of the growth unit in that direction can be determined.

3. AFM data collection and analyses

3.1. Protein preparation and crystallization

Chicken egg-white lysozyme was purchased from Sigma and repurified by cation-exchange and size-exclusion chromatography, as previously described (Ewing *et al.*, 1996). The final protein solutions were maintained at pH 4.0 with 0.1 *M* acetate buffer. Protein concentrations in these solutions were determined by UV absorbance (Aune & Tanford, 1969). Tetragonal crystals were grown in specially designed cells at ambient temperature (~293 K) from 20–40 mg ml^{-1} protein solutions with 5% NaCl. Following crystallization, the remaining protein solution was drained and the cell plate with the crystals was transferred to the AFM fluid cell. The fluid cell was then filled with fresh protein solution close to the saturation concentration. Tetragonal lysozyme solubilities were obtained from published data, which under these conditions is ~3.5 mg ml^{-1} (Cacioppo & Pusey, 1991).

3.2. Performing AFM linescans across growth steps

The details of performing AFM experiments on protein crystals, including AFM linescans, are described in other publications (Durbin & Carlson, 1992; Konnert *et al.*, 1994). All linescans were carried out at ambient temperature in the contact mode, employing a Digital Instruments Nanoscope IIIa scanning-probe microscope. Silicon nitride tips were used throughout and the scan frequency was around 20 Hz.

Regular area scans were first performed in order to identify suitable growth steps on the (110) faces of the tetragonal lysozyme crystals. The linescans were then performed across these growth steps in the [$\bar{1}$10] and the [001] directions. The protein solution concentrations were sometimes further adjusted to bring them closer to the solubility limit and the system allowed to come to an equilibrium. These precautions were necessary to ensure that the linescans were able to capture individual growth events, such as those shown in Figs. 5(*a*) and 5(*b*), rather than the continuous growth process shown in Figs. 4(*a*) and 4(*b*).

3.3. Analyzing linescan images to obtain growth-unit dimensions

An example of a raw linescan image to be analyzed is shown in Fig. 5(*a*). Although the sudden jump in the step edge when a growth event occurs is clear enough, measuring the size of this change is complicated by the variations in the location of the step edge before and after the growth event. This variation can be attributed to instrument distortions and sample drift and is similar to the variations seen in the raw data of area scans in the related AFM study (Li *et al.*, 1999). As in that study, some form of averaging has to be introduced in order to measure the change in the step edge owing to the growth event.

This was achieved by separately analyzing the height information of the sections of the image just before and just after the change. The analysis of each section showed a height peak corresponding to the growth step, and the location data was averaged over time (the *y* direction in Fig. 5*a*) in order to obtain the mean position of the step edge in the *x* direction. The difference between the averaged positions of the step edge before and after the change gives the growth-unit dimension in that direction. This analysis procedure was already available in the 'Width' function

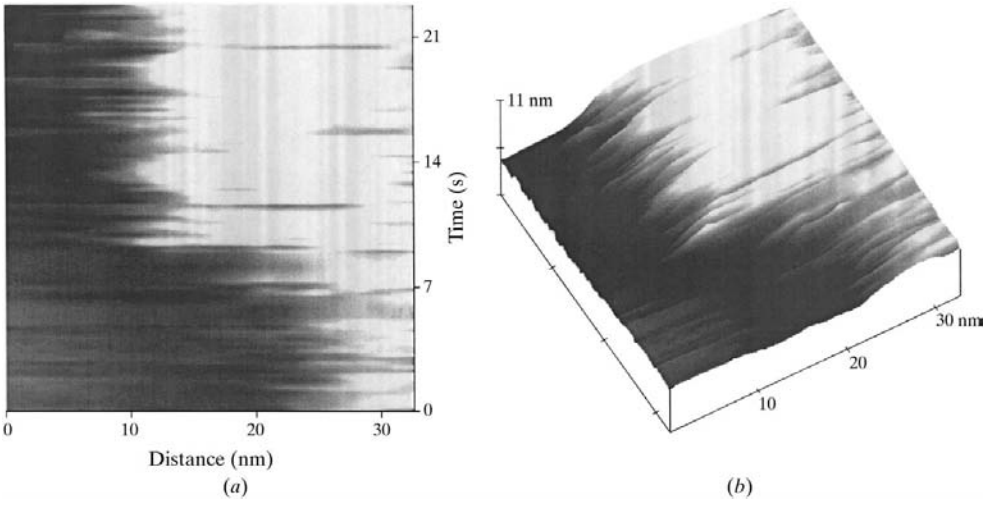

Figure 5
The (*a*) two-dimensional and (b) three-dimensional views of an AFM linescan image obtained by scanning across a growth step at very low supersaturations. The growth step, ~5.6 nm in height, is initially stationary. After about 10 s the step jumps discontinuously by ~11.2 nm, after which it remains stationary for the remainder of the linescan.

of the off-line software provided with the Nanoscope IIIa and it was not necessary to develop a specialized procedure. As part of the analysis, the standard deviation for the averaged step-edge location is also determined and displayed. Each linescan image obtained in this study was analyzed in this manner and the growth-unit dimension determined from the change in the step edge from a growth event.

4. Results and discussion

As discussed in §2, maintaining the protein solution concentration close to the solubility limit is central to observing the growth process of tetragonal lysozyme crystals as a series of discrete events. It was found that the solution protein concentration had to be extremely close to the solubility limit to achieve this. Accordingly, the protein solutions were prepared at the saturation concentration. This resulted in solutions being slightly supersaturated, slightly undersaturated or at equilibrium with the crystal for different experiments, depending on the ambient temperature. Correspondingly, the AFM linescans across the growth steps displayed growth events, dissolution events or no events at all.

Figs. 6(*a*) and 6(*b*) show the linescan images for a dissolution event and for equilibrium respectively. All collected images corresponded to one of the three events shown in Figs. 5(*a*), 6(*a*) or 6(*b*). Often, all three events occurred simultaneously at different growth steps on the same crystal face. Fig. 7 shows an image where multiple growth events occurred during a linescan experiment. This figure shows that the change in the growth step is not equal for all events, indicating that growth was proceeding on the (110) face by the addition of different-sized growth units. Figs. 5, 6 and 7 demonstrate that it is possible to observe individual growth events at the molecular level employing AFM linescans.

Many linescans were performed at the these conditions in the [$\bar{1}$10] and the [001] directions on the (110) faces. The growth-unit dimensions in both directions were determined from the linescan images, as described in the previous section, for both growth and dissolution events. Growth step heights, which correspond to the [110] direction, were also measured. These heights were found to be 5.6 nm or its multiples, implying that the growth layers and the growth units were of bimolecular height or its multiples (Fig. 2). This confirms the systematic measurements and analysis performed by Konnert *et al.* (1994). Other studies had also observed only bimolecular layers or multiples on this face (Durbin & Feher, 1990; Durbin & Carlson, 1992). This is also in agreement with our related AFM study which showed that the packing corresponding to a monomolecular layer was absent on this face (Li *et al.*, 1999).

Fig. 8 displays the distribution of growth-unit dimensions obtained from 100 linescans performed in the [$\bar{1}$10] direction. It shows that the measured dimensions cluster around the 5.6, 11.2 and 16.8 nm sizes corresponding to the bimolecular width of the 4_3 helix or its multiples. This suggests that growth units of widths corresponding to one, two or three 4_3 helices were involved in the growth process. The clear separation between the peaks indicates that growth units of one, three or five molecular widths were not involved in the growth process.

A somewhat surprising result may be the spread in the data in Fig. 8, as they imply growth-unit dimensions corresponding to fractions of molecules in some linescans. As described in §3, there are variations in the location of the growth step edge in the raw linescan images owing to instrument limitations. These are averaged out to obtain the growth-unit dimensions and a standard deviation is calculated for each dimension obtained from a linescan image. The distribution of these standard deviations for all measurements in the [$\bar{1}$10] direction are plotted in Fig. 9, and are found to have an average value of 1.2 nm. When the standard deviation for the first two peaks in Fig. 8 were determined, they were both found to be 1.0 nm. The close agreement between these standard deviations suggests that the same instrument limitations are responsible for the variations from 5.6 nm or its multiples for some growth-unit dimensions measured in this manner. If this is correct, then this AFM linescan technique will have a resolution of ~1 nm and all measured dimensions can be expected to have a distribution of sizes with a standard deviation of this magnitude.

The average value for each of the three peaks in Fig. 8, which correspond to the sizes of the three units involved in the growth process in this direction, was calculated. The results are summarized in Table 1. Despite the scatter, the average value of each peak is remarkably close to its predicted value from the widths of one, two and three 4_3 helices. For the first two peaks, each of which have at least 40 data points, the deviations do

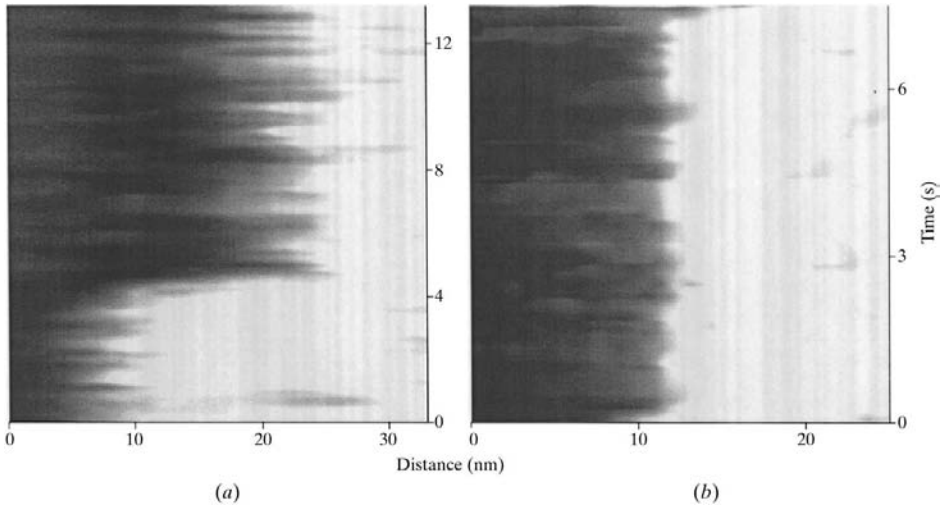

Figure 6
Linescan images showing the occurrence of other events besides growth near the saturation limit. (*a*) Image of a dissolution event which occurs after about 4 s, resulting in the growth step receding by ~11.2 nm. (*b*) Image of a stationary step.

Table 1
Growth-unit dimensions (nm).

Predicted values were obtained from the widths of 4_3 helices and averaged measured values were obtained from AFM linescans.

	Dimension in [$\bar{1}$10] direction		Dimension in [001] direction	
	Measured	Predicted	Measured	Predicted
1st peak	5.8 ± 1.2	5.6	4.1 ± 0.7	3.8
2nd peak	11.2 ± 1.2	11.2	7.7 ± 0.7	7.6
3rd peak	16.3 ± 1.2	16.8	11.6 ± 0.7	11.4

not exceed 0.2 nm. This indicates that the AFM linescan approach developed in the study can be employed to measure the growth-unit dimension accurate to less than 1 nm if a sufficient number of data points are collected.

It is clear from the above results that in the [$\bar{1}$10] direction the growth units correspond to the 4_3 helix and its multiples. As discussed in §2, this is the expected result given the observation of growth layers at least bimolecular in height on the (110) face and the 4_3 symmetry of these layers. Thus, the tetramer unit comprising a single turn of the 4_3 helix is the minimum size of a growth unit for the (110) face, as also predicted by theoretical analyses of the molecular packing (Nadarajah & Pusey, 1996; Nadarajah *et al.*, 1997; Strom & Bennema, 1997*a*,*b*). Even the observation of growth units which are multiples of the minimum bimolecular width is not surprising. Multilayer growth steps have previously been observed on the (110) face (Durbin & Feher, 1990; Durbin & Carlson, 1992; Konnert *et al.*, 1994), which should have the same growth units.

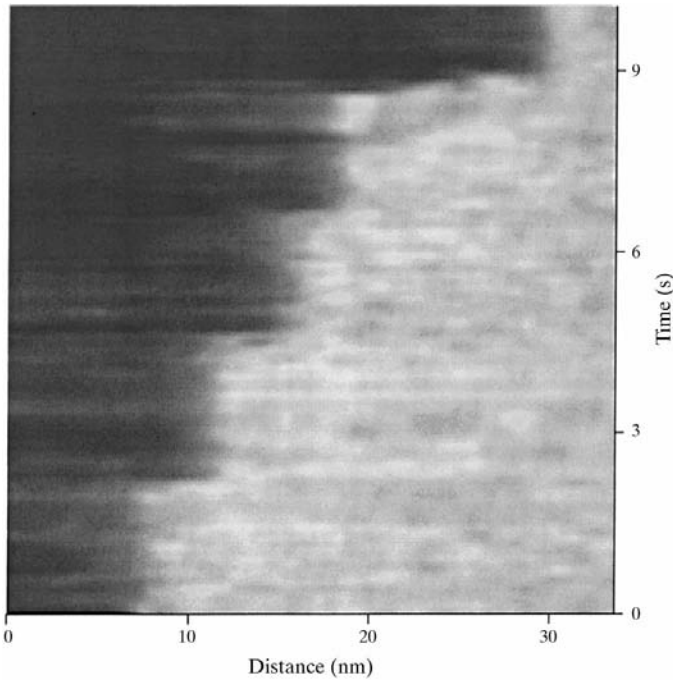

Figure 7
Linescan image showing the occurrence of four dissolution events during a single experiment. In the first three events, the step recedes by ∼5.6 nm, while in the fourth event it recedes by ∼11.2 nm.

The observation of growth units of larger than bimolecular width implies that they comprise two or more 4_3 helices. From the second and third peaks in Fig. 8, the number of such units participating in the growth process are at least equal to the number of single 4_3 helical units. This suggests that these units can produce multi-layered growth steps on the (110) face without any special mechanisms such as the poisoning of growth steps by macromolecular impurities. Poisoning by impurities had been suggested in earlier studies as the cause of these macrosteps (Durbin & Feher, 1990; Durbin & Carlson, 1992), by analogy with small-molecule crystal growth. Although an impurity-mediated mechanism cannot be ruled out, particularly for growth steps comprising many molecular layers, the results in Fig. 8 suggest that they might occur naturally and as commonly as single bimolecular layers.

Fig. 10 displays the distribution of growth-unit dimensions obtained from 65 linescans performed in the [001] direction. The measured dimensions here cluster around 3.8, 7.6 and 11.4 nm sizes, which are the lengths of growth units corresponding to one, two and three turns of the 4_3 helix, respectively. The scatter in the measurements can be expected to be the same as before, but there is less separation between the peaks here than in the [$\bar{1}$10] direction (3.8 nm *versus* 5.6 nm). This results in some overlap between the peaks in Fig. 10,

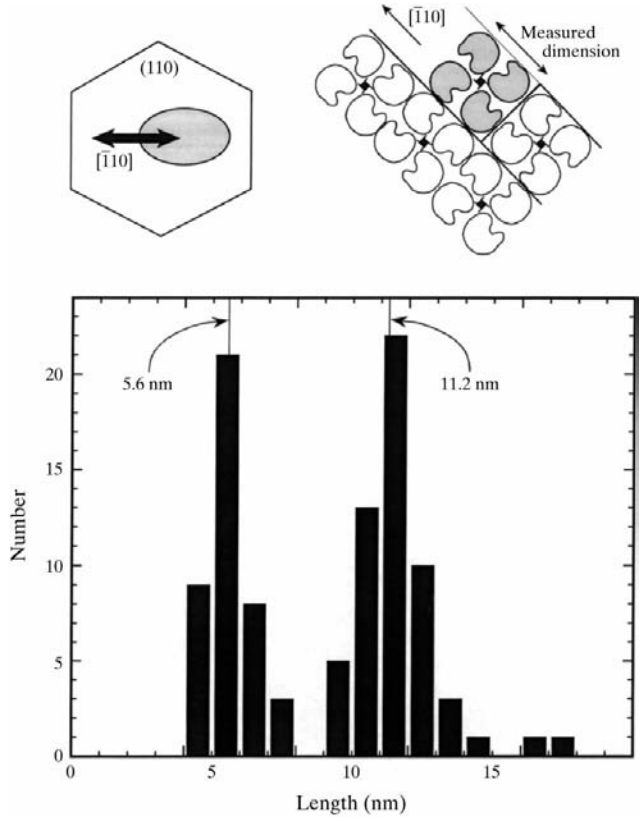

Figure 8
Distribution of growth-unit dimensions obtained from 100 linescan experiments on the (110) face. All scans were performed in the [$\bar{1}$10] direction as shown in the figure on top left. The measured dimension was the width of the growth unit as shown on the figure in top right. The dimensions corresponding to the width of single (5.6 nm) and two (11.2 nm) 4_3 helices are shown for comparison purposes.

unlike in Fig. 8. The average value from the standard deviations for each of the measurements was 0.7 nm, and the standard deviations for the first two peaks in Fig. 9 were 0.5 and 0.8 nm. The closeness of these values again indicates that the scatter in the data from predicted values largely arises from instrument limitations.

These results are summarized in Table 1. Here, too, the average values of the peaks are remarkably close to the predicted values from the lengths of 4_3 helices of one, two and three turns. For the first two peaks, each of which have at least 25 data points, the deviations do not exceed 0.3 nm. Even the third peak, which has merely ten data points, shows a deviation of only 0.2 nm.

Fig. 10 shows that most of the growth units for the (110) face comprise only a single turn of the 4_3 helix. This result, combined with the distribution of growth-unit dimensions in the $[\bar{1}10]$ direction shown in Fig. 8, indicates that the growth of the (110) face occurs by the addition of a variety of growth units. These units can vary from a minimum size of tetramers to dodecamers or larger. The only unifying aspect of these clusters is that they all correspond to one or more 4_3 helices.

The above results confirm the theoretical prediction from PBC analyses that there is an underlying molecular-level mechanism in tetragonal lysozyme crystal growth. This mechanism involves the formation of complete 4_3 helices on the crystal faces, requiring growth units of various sizes corresponding to these helices. However, the question remains as to how these growth units are formed: are they formed in solution from monomers prior to addition to the crystal face or are they directly nucleated on the surface from monomers in solution?

As discussed in §1, there is evidence that lysozyme clusters form in solution under crystallization conditions and that they correspond to the 4_3 helices. This alone would suggest that growth proceeds by the deposition of these units on the crystal faces. Furthermore, the macroscopic modeling studies have produced good agreement with the measured growth-rate data assuming this mechanism (Li *et al.*, 1995; Nadarajah *et al.*, 1997). However, these same studies also show that a significant amount of the protein remains in the monomeric state even under crystallization conditions. Additionally, other investigations seem to show that lysozyme exists only in monomeric form in solution (Muschol & Rosenberger, 1996; Gripon *et al.*, 1997). Thus, it is possible that growth could proceed by the nucleation of growth units from monomers on the crystal faces. It should be noted here that nucleation need not mean the simultaneous deposition of many lysozyme monomers to form a large growth unit. They could be formed sequentially, but at rates much faster than the millisecond time scales for performing time-resolved studies by AFM linescans.

The results of this study strongly suggest that the growth mechanism of tetragonal lysozyme crystals is by the addition of lysozyme clusters formed in solution. Although it is possible that the observed growth units could have been formed on the crystal face from monomers, not even a single such event was observed among the 165 linescans performed here. Moreover, the same aggregate growth-unit mechanism was observed for both growth and dissolution, despite the different kinetics of these processes. Finally, if tetramers and larger clusters can be nucleated on the crystal face, then the probability of such units

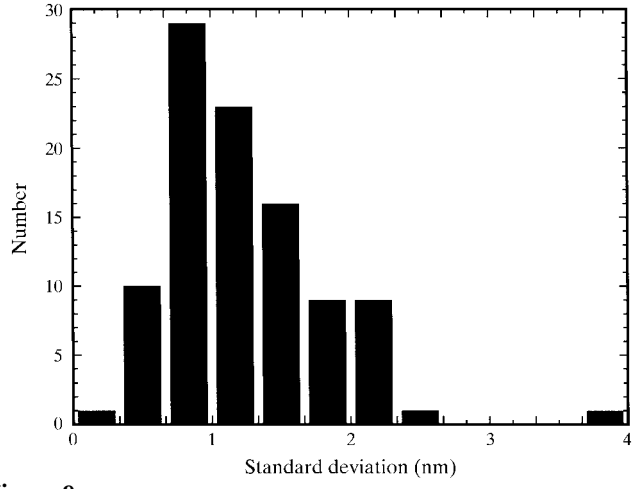

Figure 9
The distribution of standard deviations for the growth-unit dimensions obtained from all the linescans in Fig. 8. The mean value is 1.2 nm.

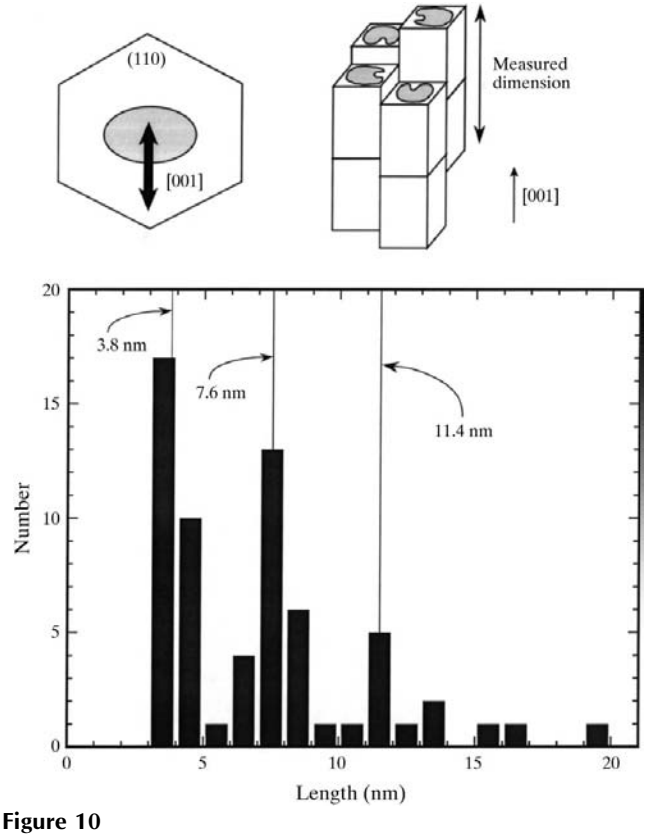

Figure 10
Distribution of growth-unit dimensions obtained from 65 linescan experiments performed in the [001] direction as shown in the figure on top left. The measured dimension was the height of the growth unit, corresponding to the number of turns of the 4_3 helix, as shown on the figure in top right. The dimensions corresponding to single (3.8 nm), two (7.6 nm) and three (11.4 nm) turns of the 4_3 helix are shown for comparison purposes.

being formed sequentially in the bulk solution are much greater.

We believe the mechanism involving lysozyme clusters in solution arises because of the two fundamental ways lysozyme crystals differ from small-molecule crystals: the non-uniformity in magnitude of molecular interactions and the maintenance of the aqueous environment in the crystal form. The implications of these differences for tetragonal lysozyme crystals were discussed in §1; namely, the formation of clusters in solution by the same interactions as in the crystal form and the requirement that the growth proceed by the completion of the 4_3 helices. In addition to this, the non-uniformity of the interactions essentially divides the growth process into two sequential steps: the formation of 4_3 helices by the strong *W* and *Z* interaction set and the attachment of these helices to each other by the weaker *X* and *Y* interaction set (Nadarajah & Pusey, 1996; Nadarajah *et al.*, 1997). The disparity in the interactions should lead to the former becoming the rapid step in the process and the latter the slow rate-determining step.

Even with the above non-uniformity in the interactions, in an inorganic system, growth would only proceed by the nucleation of the growth units on the crystal faces. This is because in such systems the non-aqueous crystalline interactions cannot be formed in the solution phase. In other words, the growth process would proceed by the slow step first followed by the rapid ones, as this is the only possible order. However, as discussed before, in protein crystals there are no such restrictions, as the crystalline interactions can be formed in solution. This means that growth will proceed by the more likely order of rapid step(s) first followed by the slow rate-determining step; that is, the formation of lysozyme clusters in solution first by the strong *W*–*Z* interaction set followed by their addition to the crystal face by the weaker *X*–*Y* interaction set.

The investigations performed here, and in the related AFM study (Li *et al.*, 1999), suggest one way which lysozyme crystal growth differs from inorganic crystal growth: there is an underlying molecular-level mechanism in addition to the classical one. Since the two causes of this difference are present to some degree in all crystals of biological macromolecules, this growth mechanism may also occur in other systems. However, if the above arguments are correct, its importance is linked to the anisotropy of the molecular interactions in the crystal. A protein with minimal differences in the magnitude of its crystalline interactions will not have a slow rate-determining step in the molecular-growth process. Crystal growth for such a protein would resemble that of inorganic crystals with growth proceeding largely by the addition of monomeric units to the crystal faces by screw dislocation/two-dimensional nucleation growth, *i.e.* by the classical crystal-growth mechanism.

Although the results presented here clearly indicate an underlying molecular-growth mechanism, further work is necessary to verify how the growth units are formed. This would require a molecular-level observation technique with time scales less than a millisecond. As noted earlier, recent advances in observing molecular-level processes, such as the photolysis of the carbon monoxide complex of myoglobin by Laue diffraction, began as more limited attempts (Teng *et al.*, 1994) which were subsequently refined (Šrajer *et al.*, 1996). It is hoped that further work on improving the time resolution of this AFM technique will also allow the question of whether the growth units are formed in solution or nucleated on the crystal face to be conclusively resolved.

5. Conclusions

This study has shown that there is an underlying molecular-level growth mechanism for the (110) face of tetragonal lysozyme crystals to the classical mechanism involving screw dislocation/two-dimensional nucleation growth. This mechanism involves the addition of a variety of growth units, which are lysozyme clusters corresponding to the 4_3 helix, to the crystal face. In the $[\bar{1}10]$ direction, the size of the growth units correspond to the width of the 4_3 helix or its multiples. In the [001] direction, they correspond to single or multiple turns of this helix. These results are in agreement with theoretical predictions from PBC analyses (Nadarajah & Pusey, 1996; Nadarajah *et al.*, 1997; Strom & Bennema, 1997*a*,*b*) and earlier experimental observations (Durbin & Feher, 1990; Durbin & Carlson, 1992; Konnert *et al.*, 1994). The AFM linescan technique employed here could not resolve the issue of whether these growth units are formed in solution from monomers prior to addition to the crystal face or are directly nucleated on the surface from monomers in solution. However, the results suggest the former mechanism.

The linescan technique developed here represents a new application for atomic force microscopy. It can be employed for time-resolved investigations of other molecular processes which occur on, or can be slowed down to, the millisecond timescale. It is also possible to measure molecular dimensions of particular changes during the process, up to a resolution of less than 1 nm, if a sufficient number of data points are collected. Although it can currently only be used for processes with a time scale of at least 1 ms, it is hoped further refinements will improve its time resolution.

This work was supported by NASA grant NCC8-134 to the University of Toledo. Support was also provided by the University of Toledo.

References

Aune, K. C. & Tanford, C. (1969). *Biochemistry*, **8**, 4579–4590.
Banerjee, S. K., Poglotti, A. & Rupley, J. A. (1975). *J. Biol. Chem.* **250**, 8260–8266.
Behlke, J. & Knespel, A. (1996). *J. Cryst. Growth*, **158**, 388–391.
Cacioppo, E. & Pusey, M. L. (1991). *J. Cryst. Growth*, **114**, 286–292.
Chernov, A. A. (1984). *Crystal Growth.* Berlin: Springer.
Durbin, S. D. & Carlson, W. E. (1992). *J. Cryst. Growth*, **122**, 71–79.
Durbin, S. D. & Feher, G. (1990). *J. Mol. Biol.* **212**, 763–774.
Ewing, F. L., Forsythe, E. L., van der Woerd, M. & Pusey, M. L. (1996). *J. Cryst. Growth*, **160**, 389–397.
Gripon, C., Legrand, L., Rosenman, I., Vidal, O., Robert, M. C. & Boue, F. (1997). *J. Cryst. Growth*, **178**, 575–584.
Hampe, O. G., Tondo, C. V. & Hasson-Voloch, A. (1982). *Biophys. J.* **40**, 77–82.

Konnert, J. H., D'Antonio, P. & Ward, K. B. (1994). *Acta Cryst.* D**50**, 603–613.
Kuznetsov, Yu. G., Malkin, A. J., Glantz, W. & McPherson, A. (1996). *J. Cryst. Growth*, **168**, 63–73.
Li, H., Perozzo, M. A., Konnert, J. H., Nadarajah, A. & Pusey, M. L. (1999). *Acta Cryst.* D**55**, 1023–1035.
Li, M., Nadarajah, A. & Pusey, M. L. (1995). *J. Cryst. Growth*, **156**, 121–132.
Malkin, A. J., Kuznetsov, Yu. G., Glantz, W. & McPherson, A. (1996). *J. Phys. Chem.* **100**, 11736–11743.
Malkin, A. J., Kuznetsov, Yu. G., Land, T. A., DeYoreo, J. J. & McPherson, A. (1995). *Nature Struct. Biol.* **2**, 956–959.
Malkin, A. J., Kuznetsov, Yu. G. & McPherson, A. (1996*a*). *Proteins*, **24**, 247–252.
Malkin, A. J., Kuznetsov, Yu. G. & McPherson, A. (1996*b*). *J. Struct. Biol.* **117**, 124–137.
Minezaki, Y., Nimura, N., Ataka, M. & Katsura, T. (1996). *Biophys. Chem.* **58**, 355–363.
Muschol, M. & Rosenberger, F. (1996). *J. Cryst. Growth*, **167**, 738–747.
Nadarajah, A., Forsythe, E. L. & Pusey, M. L. (1995). *J. Cryst. Growth*, **151**, 163–172.
Nadarajah, A., Li, M. & Pusey, M. L. (1997). *Acta Cryst.* D**53**, 524–534.
Nadarajah, A. & Pusey, M. L. (1996). *Acta Cryst.* D**52**, 983–996.
Pusey, M. L. (1991). *J. Cryst. Growth*, **110**, 60–65.
Sophianopoulos, A. J. (1969). *J. Biol. Chem.* **244**, 3188–3193.
Šrajer, V., Teng, T.-Y., Ursby, T., Pradervand, C., Ren, Z., Adachi, S.-I., Schildkamp, W., Bourgeois, D., Wulff, M. & Moffat, K. (1996). *Science*, **274**, 1726–1729.
Strom, C. S. & Bennema, P. (1997*a*). *J. Cryst. Growth*, **173**, 150–158.
Strom, C. S. & Bennema, P. (1997*b*). *J. Cryst. Growth*, **173**, 159–166.
Studebaker, J. F., Sykes, B. D. & Wien, R. (1971). *J. Am. Chem. Soc.* **93**, 4579–4585.
Teng, T.-Y., Šrajer, V. & Moffat, K. (1994). *Nature Struct. Biol.* **1**, 701–705.
Vekilov, P. G., Ataka, M. & Katsura, T. (1993). *J. Cryst. Growth*, **130**, 317–320.
Vekilov, P. G. & Rosenberger, F. (1996). *J. Cryst. Growth*, **158**, 540–551.
Vidal, O., Robert, M. C. & Boue, F. (1998). *J. Cryst. Growth*, **192**, 257–270.
Wilcox, F. H. & Daniel, L. J. (1954). *Arch. Biochem. Biophys.* **52**, 305–312.
Williamson, J. C., Cao, J., Ihee, H., Frey, H. & Zewail, A. H. (1997). *Nature (London)*, **386**, 159–162.
Wilson, L. J., Adcock-Downey, L. & Pusey, M. L. (1996). *Biophys. J.* **71**, 2123–2129.
Wilson, L. J. & Pusey, M. L. (1992). *J. Cryst. Growth*, **122**, 8–13.
Zehavi, U. & Lustig, A. (1971). *Biochim. Biophys. Acta*, **236**, 127–130.
Zewail, A. H. (1996). *J. Phys. Chem.* **100**, 12701–12724.